Multiple scattering theory of electron transport in disordered metals in the muffin-tin potential model. III. Numerical results

1990 J. Phys.: Condens. Matter 2 8827

(http://iopscience.iop.org/0953-8984/2/44/011)

J. Phys.: Condens. Matter 2 (1990) 8827–8840. Printed in the UK

Multiple scattering theory of electron transport in disordered metals in the muffin-tin potential model: III. Numerical results

R Frésard†, H Beck† and M Itoh‡

† Institut de Physique, Université de Neuchâtel, CH-2000 Neuchâtel, Switzerland

‡ Department of Physics, Shimane University, Matsue 690, Japan

Received 14 June 1990

Abstract. A model calculation is attempted for the electrical resistivity and the electronic density of states of liquid and amorphous metals using the muffin-tin EMA formalism developed by the present authors. A single s-phase shift model is adopted here with different scattering strengths. It is found that the short- and the medium-range order in the atomic structure causes a deep minimum in the electronic density of states and, furthermore, a very sharp rise of the resistivity when the Fermi energy approaches the minimum. It causes in turn a strong temperature dependence of resistivity for strong scattering cases through the temperature dependence of the Fermi–Dirac distribution function. The temperature dependence also comes from the structure factor, and both effects support the Mooij correlation between the resistivity and the temperature coefficient of resistivity.

1. Introduction

In the preceding papers (Itoh *et al* 1989, 1990; to be referred to as I and II respectively) we have developed a formal theory of electron transport of disordered metals by extending the work by Roth and Singh (1982). The theory is based upon the effective medium approximation (EMA), introduced originally by Roth (1974), and includes both the multiple scattering processes and the structural effect in a self-consistent way. It is emphasized in particular that it is capable of dealing with the strong scattering materials including the d- or f-electrons and also that both the electronic density of states and the transport are treated on the same footing. Its application is therefore extremely interesting in connection with the recent experimental activities on high resistivity metallic glasses (see, for a review, Howson and Gallagher 1988) and on many simple metallic glasses in which a strong Fermi surface–Brillouin zone interaction is suggested (Häussler and Baumann 1983, Mizutani 1983). In particular the latter systems clearly show the interplay between the short-range order and the various anomalies in the transport properties, which is most likely related to the observed minimum in the density of states, thus providing physically very attractive problems. In the present paper we attempt an application of the theory to a system of hard sphere scatterers with s-phase shifts, in order to elucidate the interplay mentioned above. We calculate the density of states and the resistivity for a fixed atomic configuration. Therefore the effect of the electronic states on the structure (Häussler 1983) is neglected and we concentrate only

0953-8984/90/448827 + 14 $03.50

on the study of the scattering mechanism. Although the model is quite suitable for simple metals, we vary the phase shift up to the strong scattering case in order to get an insight into the non-simple materials. We also vary the packing fraction to investigate the structure effect. The temperature dependence of the resistivity is studied by taking into account the finite width of $(-\mathrm{d}f/\mathrm{d}E)$, the derivative of the Fermi–Dirac distribution function, the effect of which may be quite substantial as reported recently (Zhao and Ching 1989). Since the temperature dependence of the resistivity is related to many other factors (in particular the temperature dependence of the structure, which causes in turn a change in the Fermi level), it is not quite possible to give a definite conclusion at this stage. Yet we will see that our calculation is consistent with the Mooij correlation. Moreover it shows that there are many aspects of the static effects we should study before we discuss the dynamical effects on the temperature dependence of resistivity.

In the next section we start with a brief summary of the formalism for a single-component system with s-scattering. The equations become relatively simple in this case. For the mathematical details to include the higher angular momentum phase shifts, paper II should be consulted. In section three we present the result of numerical calculations for the density of states, resistivity, and the spectral functions. A deep minimum in the density of states is observed for strong scattering cases. It is seen to be related to the wiggling curve of the dispersion relation with quasi-particle damping width, which shows the strong Fermi surface–Brillouin zone interaction discussed by Häussler and Baumann (1983). The resistivity has very high values there, far exceeding the Ziman contribution. The importance of the vertex corrections is emphasized and the temperature dependence of resistivity is also discussed. The final section is devoted to further discussions.

Some of the results have been summarized in the proceedings of LAM 7 (Frésard *et al* 1990) and more details are given in a doctoral thesis (Frésard 1989).

2. Summary of the formalism for s-scattering

As emphasized in the introduction, we are able to calculate both the electronic density of states and the transport properties on equal footings. For this we need to solve two levels of equations. The first level is a set of coupled equations for one-electron properties:

$$\tilde{G}_k(\kappa) = \tilde{B}_k(\kappa) + \int \frac{q^2\,\mathrm{d}q}{2\pi^2 n} a_0(k,q)\tilde{G}_q(\kappa)Q_q(\kappa,\kappa)\tilde{G}_q(\kappa) \tag{1.1}$$

$$T_d(\kappa,\kappa) = t(\kappa,\kappa) + t(\kappa,\kappa)\int \frac{k^2\,\mathrm{d}k}{2\pi^2}\tilde{G}_k(\kappa)Q_k(\kappa,\kappa)B_k(\kappa)T_d(\kappa,\kappa) \tag{1.2}$$

$$Q_k(\kappa,\kappa) = nT_d(\kappa,\kappa) + nT_d(\kappa,\kappa)\tilde{G}_k(k)Q_k(\kappa,\kappa). \tag{1.3}$$

In the above equations $t(p,p')$ is the matrix element for the single scattering centre, whereas $Q_k(p,p')$ is the quantity representing the total T-matrix of the system, with k representing the ionic momentum, and $T_d(p,p')$ is its diagonal part (in this paper we used $nT_d(\kappa,\kappa)$ instead of Q_d used in paper I). The arguments in the parenthesis are for the electron momentum variable but only the on-shell components appear in the above equations; namely $p = p' = \kappa$, where κ is defined by $\kappa = \sqrt{E}$. The quantities B, $\tilde{B}$ are defined as follows:

$$B_k(\kappa) = 1/(\kappa^2 - k^2 + i\varepsilon) \tag{1.4}$$

$$\tilde{B}_k(\kappa) = B_k(\kappa) + \int \frac{q^2\,dq}{2\pi^2 n} a_0(k, q) B_q(\kappa). \tag{1.5}$$

The function $a_0(k, k')$ is defined as the $l = 0$ component of the following expansion

$$h(|\boldsymbol{k} - \boldsymbol{k}'|) = 4\pi\Sigma_L Y_L(\boldsymbol{k}) a_l(k, k') Y_L(\boldsymbol{k}') \tag{1.6}$$

with $h = g - 1$ being the total correlation function. The remaining quantity, $\tilde{G}(p, p')$, is the normalized propagator defined diagrammatically in I and is an important building block of the theory. The electron self energy Σ is obtained through the following relation:

$$\Sigma(k) = [Q_k(k, k)/(1 + B_k(\kappa) Q_k(k, k))] \tag{1.7}$$

Note that the self energy is related not only to the solution of the on-shell equations but also to the off-shell component of the T-matrix. This is because the self energy includes detailed information on the electronic states, although the information about the distribution of the eigenstates, i.e. the density of states, is fully included in the on-shell component (Lloyd 1967). The equations (1.1)–(1.3) only determine the on-shell components of the relevant quantities. The off-shell components are obtained easily from the following relations:

$$T_d(p, p') = \frac{t(p, p')\tau - t(p, \kappa)t(\kappa, p')}{\tau} + \frac{t(p, \kappa)}{\tau} T_d(\kappa, \kappa) \frac{t(\kappa, p')}{\tau} \tag{1.8}$$

$$Q_k(p, p') = n \frac{t(p, p')\tau - t(p, \kappa)t(\kappa, p')}{\tau} + \frac{t(p, \kappa)}{\tau} Q_k(\kappa, \kappa) \frac{t(\kappa, p')}{\tau}. \tag{1.9}$$

Finally the density of states and the spectral functions are obtained from the configurationally averaged Green function

$$\langle G(k) \rangle = 1/(G_0(k) - \Sigma(k)) = G_0(k) + G_0(k) Q_k(k, k) G_0(k). \tag{1.10}$$

Some caution is required in solving the equations because it contains free electron divergences in B, $\tilde{B}$. We are able to rewrite the whole equations in a divergence-free form; the details are given in the appendix. Solving our integral equations is a highly non-linear problem. As for the calculation of the resistivity, the problem is basically linear after having solved the one-electron problem. In the case of the EMA this contribution is conveniently integrated into the formalism and we obtain the following expression for the DC conductivity:

$$\sigma = \int dE \left(-\frac{\partial f}{\partial E} \right) \sigma(E) \tag{1.11a}$$

$f(E)$ being the Fermi function and the differential conductivity $\sigma(E)$ being determined by (suppressing, for simplicity, the energy argument E):

$$\sigma = \frac{\hbar}{3\pi} \left(\frac{e\hbar}{m} \right)^2 \int \frac{k^3\,dk}{2\pi^2} \left(G_0^+(k) G_0^-(k) X^{+-}(k) - \frac{m}{\hbar^2} \mathrm{Re} \left(G^+(k)^2 \frac{d\Sigma^+(k)}{dk} \right) \right)$$

$$+ \frac{\hbar}{3\pi} \left(\frac{e\hbar}{m} \right)^2 \int k^4\,dk\, A(k)^2 \tag{1.11b}$$

where $A(k, E) = -\operatorname{Im} G^{+}(k, E)$ is the spectral function and G_0^+, G_0^- are the free electron propagators. The X^{+-} term represents the vertex corrections for the electron–hole pair given by

$$X^{+-}(k) = \left|\frac{t(k,k)}{\tau} Q_k(\kappa,\kappa)\right|^2 X_1^{+-}(k) + 2\,\mathrm{Re}\left(\frac{t(k,\kappa)}{\tau} Q_k(\kappa,\kappa) X_2^{+-}(k,k)\right) + X_3^{+-}(k) \tag{1.12}$$

where

$$X_1^{+-}(k) = \int \frac{p^2\,\mathrm{d}p}{2\pi^2 n} a_1(k,p)\left(G_0^+(p) p G_0^-(p)\left|\frac{t(p,\kappa)}{\tau}\right.\right.$$
$$\left.\left.\times \frac{Q_p(\kappa,\kappa)}{nT_d(\kappa,\kappa)}\right|^2 + \left(\frac{Q_p(\kappa,\kappa)}{nT_d(\kappa,\kappa)} - 1\right) X_1^{+-}(p)\right) \tag{1.13}$$

$$X_2^{+-}(k,k') = \int \frac{p^2\,\mathrm{d}p}{2\pi^2 n} a_1(k,p)\left[\frac{t(p,k)}{\tau}\frac{Q_p(\kappa,\kappa)}{nT_d(\kappa,\kappa)}\right.$$
$$\times G_0^+(p) p G_0^-(p)\frac{n(t(k',p)\tau - t(\boldsymbol{k}',\kappa)t(\kappa,p))}{\tau}$$
$$\left.\times\left(\frac{Q_p(\kappa,\kappa)}{nT_d(\kappa,\kappa)} - 1\right) X_2^{+-}(p,k')\right] \tag{1.14}$$

$$X_3^{+-}(k) = \int \frac{p^2\,\mathrm{d}p}{2\pi^2} a_1(k,p) G_0^{\pm}(p)\left|\frac{n(t(k,p)\tau - t(k,\kappa)t(\kappa,p))}{\tau}\right|^2. \tag{1.15}$$

In the above equations τ is the on-shell component $t(\kappa,\kappa)$ of the single scatterer t-matrix and $a_1(k,k')$ is the $l=1$ component appearing in the expansion (1.6). The vertex corrections to the particle–particle (or hole–hole) pair are already included in (1.11). This term, together with the large wavenumber contributions to the particle–hole vertex corrections, forms the effective mass and the scattering rate renormalizations (Itoh and Watabe 1984a).

3. Results

We have used the spherical square-well potential for our muffin-tin potential. The radius and the depth of the potential are denoted by a and V_0 respectively, for which we have chosen $V_0a^2 = 0.9$, $V_0a^2 = 1.9$ and $V_0a^2 = 2.4$. Our unit is $\hbar = 2m = e^2 = 1$. For these parameters bound states are not yet formed. The expressions for the t-matrix elements for this potential are given by Kujawski and Lambert (1973) and by Fuda and Whiting (1973). The hard sphere system is used to describe the atomic structure, and we use the analytic solution of the Percus–Yevic equation for the structure factor. We have studied the three cases of the packing fraction, $\eta = 0.42$, 0.45 and 0.47. The atomic density is fixed to be $n = \sqrt{2}$, which means that the nearest-neighbour distance is set equal to unity for the FCC structure. We also fix the ratio of the hard sphere radius to the muffin-tin

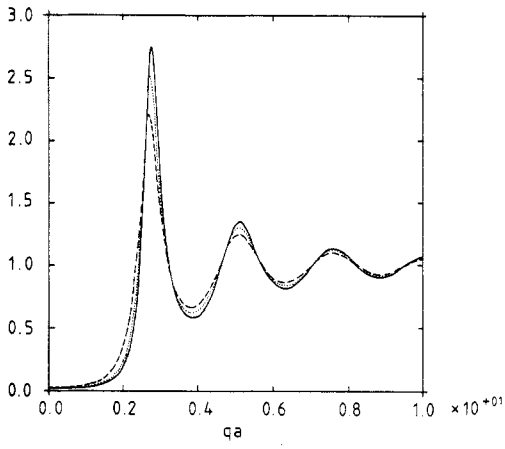

Figure 1. Hard sphere structure factor used in our calculations with the following packing fractions: $\eta = 0.42$ (broken curve), $\eta = 0.45$ (dotted curve), $\eta = 0.47$ (full curve).

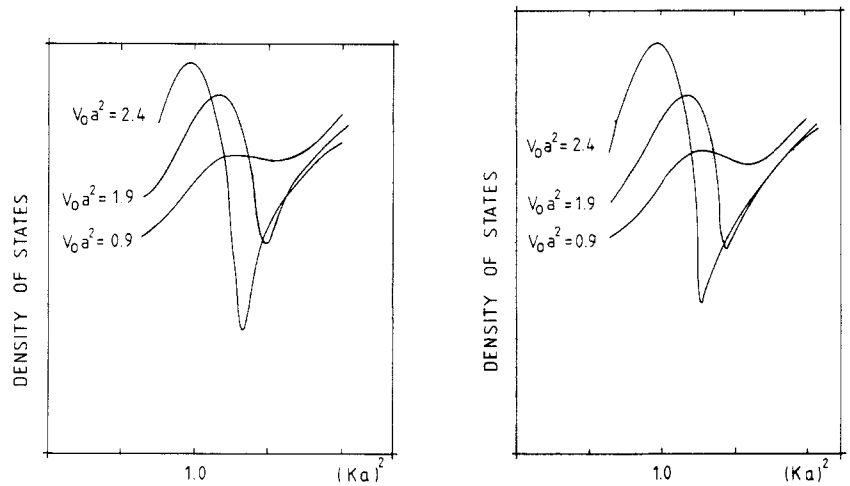

Figure 2. Electronic density of states (in arbitrary units) in the vicinity of the minimum for two different packing fractions (*a*): $\eta = 0.45$, (*b*): $\eta = 0.47$ and three potential strengths (indicated on the figures).

radius to be 1.25, so that the muffin-tin spheres do not overlap. The structure factors used for our calculations are plotted in figure 1

3.1. Density of states: structure induced minimum

First we show the results of the DOS calculation. In figure 2 the DOS curves are plotted for various scattering strengths at fixed atomic structure. The minimum of the DOS is already seen in the case of $V_0a^2 = 0.9$, becoming more and more pronounced for stronger scattering. The intermediate value, $V_0a^2 = 1.9$, already corresponds to a strong scattering metal in terms of the resistivity value, if the Fermi level is close to the minimum of the DOS (see below). For $V_0a^2 = 2.4$ the minimum is very deep. It is not clear whether a real band gap is created by s-phase shift alone before we start to have the bound states

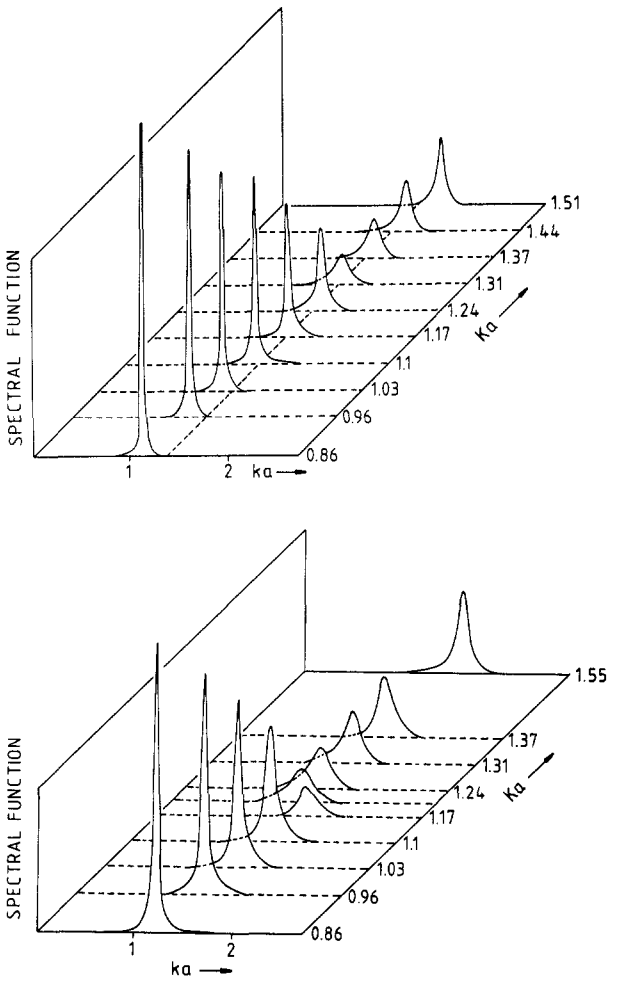

Figure 3. Electronic spectral functions, plotted (in arbitrary units) as a function of wavenumber (ka) for various values of κa. The packing fraction is $\eta = 0.47$ and the potential strengths are (*a*) $V_0a^2 = 1.9$ and (*b*) $V_0a^2 = 2.4$.

(see below for a cluster calculation for s- and p-phase shifts). However it is concluded from the behaviour of the spectral functions that the minimum is produced by the 'Bragg scattering' at the zone-boundary. In figures 3 and 4 we have plotted the spectral functions and the dispersion relation respectively for $V_0a^2 = 1.9$, the latter of which has been derived from the peak positions of the former. As is seen from figure 3 the peaks of the spectral functions are very sharp for low energies. The width of the peak is shown by the hatches in figure 4. When the wave number k approaches $k_p/2$, where k_p is the peak position of the structure factor, the peak becomes broadened, and it becomes sharp again for higher k values. The effective dispersion relation is seen to have a wiggling form around $k = k_p/2$. We see therefore that the spectral function has a double-peak structure when the plot is made against the energy for a fixed k, although a finite magnitude is observed between the two peaks. All these features are, of course, due to the reminiscence of the gap formation mechanism by Bragg reflection in the presence

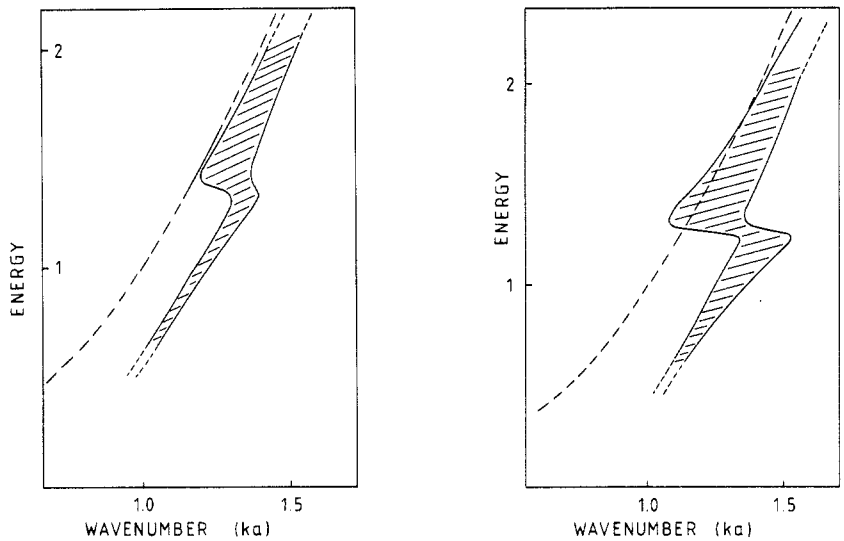

Figure 4. The effective dispersion relation for $\eta = 0.47$ and the potential strengths (*a*) $V_0a^2 = 1.9$ and (*b*) $V_0a^2 = 2.4$. The broken curve locates the free electron energy $E = \hbar^2k^2/2m$ and the hatched area indicates the width of the spectral function.

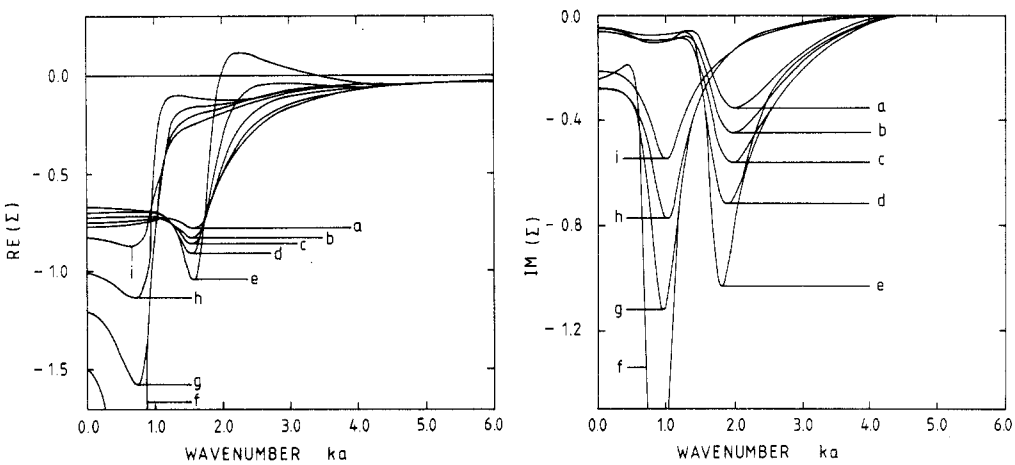

Figure 5. Electronic self-energy (*a*): real part, (*b*): imaginary part for various energies E. a: 0.739, b: 0.927, c: 1.06, d: 1.21, e: 1.37, f: 1.53, g: 1.71, h: 1.89, i: 2.39.

of the short range order. On the other hand, however, the figure also shows that the same mechanism can enhance the total scattering effect when the potential is not very weak and when the system is not in a perfect order, as represented by the broad width near the 'zone boundary'.

It may be interesting to see how the shape of the spectral function (being the imaginary part of the Green function (1.10)) is formed by the self-energy Σ. Figure 5 shows the real and imaginary part of Σ as a function of wave number for various energies.

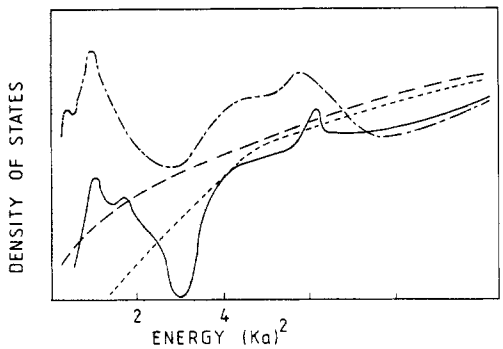

Figure 6. Density of states of a 13 atom FCC cluster taking into account s- and p-phase shifts (V_0a^2 = 5). The broken curve gives the free electron result for comparison, the dotted and chain curves are for s- and p-scattering alone respectively (the other phase shift being put equal to zero) and the final curve shows the density of states for s- and p-scattering.

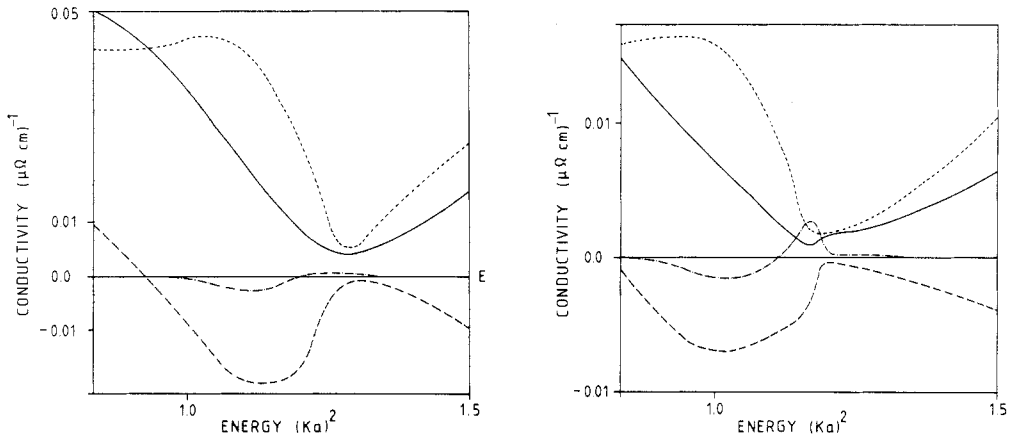

Figure 7. Contributions to the electrical conductivity (*a*): V_0a^2 = 1.9; (*b*): V_0a^2 = 2.4. The packing fraction is η = 0.47. Dotted curve: spectral contribution (see text), broken curve: contribution from X_1^-, chain curve: contributions from the second term in (1.11b) involving the derivative of $\Sigma(k)$. The total conductivity is given by the full curve.

There is a 'jump' between the energy values E = 1.37 and E = 1.53, which is responsible for the two-peak structure of the spectral function mentioned above.

For the sake of comparison we also show in figure 6 the density of states curves calculated for 13 s- and p-scatterers arranged on an FCC structure (V_0a^2 = 5). Here it is the p-scattering which yields a strong structure induced minimum (see the chain curve) which, when combined with s-scattering, leads to a real gap in the spectrum (full curve). (More details about cluster calculations can be found in Frésard and Beck (1986) and Beck *et al* (1987)).

3.2. Residual resistivity

In figure 7 plots are made for the conductivity function, $\sigma(E)$, for V_0a^2 = 1.9 and 2.4 for a fixed configuration of η = 0.47. These plots show the conductivity of degenerate electrons and are considered to be the inverse of the residual resistivity in the case of amorphous metals. Three contributions are shown separately in the figure, corresponding to the three terms in (1.11b). The total conductivity is shown by the full

curves. The spectral contributions, which are given by neglecting the difference between $\langle GG \rangle$ and $\langle G \rangle \langle G \rangle$, are shown by the dotted lines. There are also two types of vertex corrections, namely the corrections for the particle–hole pair and for the particle–particle pair, represented by the broken lines and by the chain lines respectively. The results include the off-shell contributions in the complex form, the major part of which being absorbed in the 'conventional term', i.e. in the contribution from X_1^{+-} (see paper I). The contributions from X_2^{+-} and X_3^{+-} are invisibly small in the figures.

A very sharp drop of the conductivity is observed near the DOS minimum in both figures. This clearly shows that the same scattering mechanism governs both the DOS and the conductivity function. It is emphasized that the vertex corrections are as important as the spectral contributions. The correction from the particle–hole pair has large negative values except at the very bottom of the minimum (in the low energy region it is seen to change its sign). The correction from the particle–particle pair is also seen to be very substantial when the potential is strong. It is notable that it changes its sign when we pass through the minimum. This is because it is related to the dispersion effect, corresponding to the effective-mass correction (see Itoh and Watabe 1984, Itoh 1985), which must have opposite signs on both sides of the 'zone boundary'. Our calculation shows that the particle–particle contributions can by no means be neglected, although they are ignored in most theoretical calculations, including the recent treatments of the quantum interference effect. All three contributions are strongly affected by the damping effect around the minimum, the magnitude of the total conductivity being thus reduced dramatically.

It should be noted that the particle–hole vertex correction has positive values in the low-energy region, where the spectral functions have sharp peaks and therefore the weak scattering picture holds. This behaviour of the corrections manifests the importance of the transition-rate renormalization discussed by Itoh and Watabe (1984b). Without renormalization the angular dependence of the scattering probability is determined solely by the structure factor because, in the present model, the individual scatterer causes only isotropic s-scattering. Then the slope of the structure factor is the only responsible factor for the sign of the vertex corrections. In the present case the slope is positive and, accordingly, the negative sign of the correction should be obtained. The only possible answer to this puzzle is that in the weak scattering domain the scattering is not really weak in the sense of the NFE approximation, but the 'quasi-particle states' are formed due to renormalization. The transition rates between these renormalized states are expected to have very different angular dependence. This corresponds to the contributions from the large k values beyond the quasi-particle peak, discussed by Itoh and Watabe (1984b). Namely, the quasi-particle state is not a simple free electron state but a superposition of many plane waves of the wide range of wave numbers surrounding the peak. Clearly this cannot be treated by the Ziman type of approach in which only the structural information below $2k_F$ is incorporated. The comparison to the Ziman formula is made in figure 8 in terms of resistivity. It is seen that near the minimum of the DOS the Ziman approach is no more accurate and the difference between the two theories is never small even for the weakest potential of $V_0a^2 = 0.9$.

3.3. Temperature coefficient of resistivity (TCR)

So far we have only been concerned about the conductivity of degenerate electrons for a fixed configuration. Although such calculations can include the temperature effect by using the observed structure factor at a given temperature, one needs to be careful

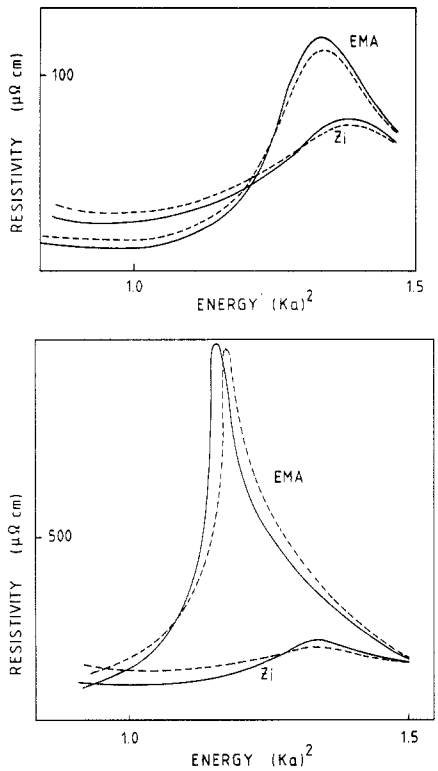

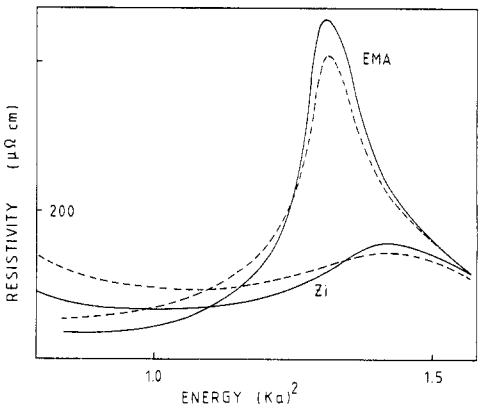

Figure 8. Resistivity as a function of energy (a): $V_0a^2 = 0.9$; (b): $V_0a^2 = 1.9$; (c): $V_0a^2 = 2.4$. The full curves are for the higher packing fraction ($\eta = 0.47$), the broken curves for the lower one ($\eta = 0.42$). The two pairs of curves show the result for Ziman lowest order perturbation theory (Zi) and for the full EMA calculation.

in dealing with this problem in the following points. There are at least three major factors which are responsible for the temperature dependence of resistivity of liquid or amorphous metals, even though we limit ourselves to the elastic scattering conduction. The first is that, as in the Ziman formula, the temperature effect comes in directly through the structure factor. In our theory this occurs in two ways; firstly the structure factor affects both the one-electronic self energy and the transport processes and secondly the position of the Fermi level for a given carrier number is temperature dependent; the Fermi level is determined only after we have calculated the DOS using the structure at a given temperature. Finally, we must bear in mind that the electrons are not really degenerate at finite temperature and one must carry out the energy integration of (1.11a) without replacing $(-\mathrm{d}f/\mathrm{d}E)$ by a delta function. The latter point is usually neglected for metals. However, its importance has been emphasized recently by Zhao and Ching (1989), and we shall investigate this point first. We have plotted in figure 9 the resistivity values for $V_0\,a^2 = 1.9$ and $\eta = 0.47$ against the temperature T, for Fermi energies lying near the minimum of $\sigma(E)$, by integrating expression (1.11a). Our plot shows that the effect of 'smearing out' through the derivative of the Fermi–Dirac function gives a negative TCR which has the right order of magnitude for typical strong scattering metals, namely $(I/\rho)(\partial\rho/\partial T) \approx 10^4\,\mathrm{K}^{-1}$ (see Howson and Gallagher 1988).

This contribution to TCR should be negative whenever we have a deep minimum of $\sigma(E)$ around the Fermi level, a situation emphasized by Zhao and Ching (1989). By applying the Sommerfeld expansion to evaluate the integral (1.11a) the quadratic dependence on T is obtained. However our minimum is so deep that this approximation is not

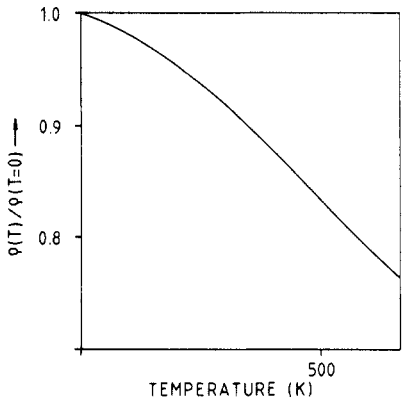

Figure 9. Resistivity, as a function of temperature, for $V_0a^2 = 1.9$ and $\eta = 0.47$, as obtained from expression (1.11a).

accurate enough. Since the minimum is created by the Bragg reflections, it is very tempting to conclude that the negative TCR can be caused by the strong Fermi surface–Brillouin zone interaction. This tendency is along the direction of the Mooij correlation and it would certainly explain some cases.

As to the first point we can attempt to find a qualitative argument by comparing the resistivity between different packing fractions for a fixed potential strength. Figure 8 shows such plots for $\eta = 0.42$ and 0.47 (the effect of $\partial f/\partial E$ is not included in these plots). It is seen from the figure that the resistivity can be higher for the higher packing fractions in some energy regions. For the weak potential, $V_0a^2 = 0.9$, we have a negative TCR when the resistivity $\rho(E)$ exceeds 50 $\mu\Omega$ cm. The cross-over from positive to negative TCR occurs at a higher ρ value ($\approx$200 $\mu\Omega$ cm) for $V_0a^2 = 2.4$, the strongest scattering case considered, the cross-over occurs again at about the same ρ value on the low energy side of the resistivity peak. It shows, however, the opposite tendency on the high energy side. In this case the main effect of changing η seems to be the shift of the deep minimum in $D(E)$, see figure 2, which produces a similar shift in the resistivity versus energy curve. By estimating the difference of 0.05 in the packing fraction η to correspond approximately to 500 K in temperature the magnitude of the negative TCR, obtained in our calculations again seems to be of the typical order of magnitude observed experimentally in highly resistive disorder metals.

We have not investigated the second point. However, a shift of the Fermi-level with temperature in the vicinity of the minimum may yield a significant effect on the temperature dependence of resistivity. This is anticipated in connection with the last point because the width of the deep minimum of $\sigma(E)$ for the strong scattering case is of the order of the room temperature. Therefore highly self-consistent calculations are required for both the DOS and the conductivity function to study the temperature effect quantitatively. At present our EMA transport theory is the only analytic theory with this self-consistency (Itoh *et al* 1984a). The investigation is not difficult in EMA because the expression for the integrated DOS is available (Niizeki 1979, Huisman *et al* 1981).

4. Summary and discussion

We have presented a first coherent theoretical description of the density of states *and* the resistivity of a model disordered metal using muffin-tin EMA formalism. It is shown

to be the most proper extension of the KKR-CPA formalism (see, for a review, Ehrenreich and Schwartz 1976), which has been highly successful for the substitutionally disordered alloys, to the structurally disordered metals (see, e.g. Yonezawa *et al* 1975). We would like to call for particular attention to this point; although the basic formalism was completed some years ago (Roth and Singh 1982) the above point does not seem to be well known. This is partly because of its mathematical complexity. Also the original formalism appears to be intractable due to the off-shell contributions. The off-shell corrections have been included in the complete form in I and II, and evaluated in the present paper. The main obstacle in the Roth–Singh formalism has thus been overcome.

Our calculation elucidated the strong effect of Bragg reflection in the vicinity of $k = k_p/2$ and the importance of the interplay between the multiple scattering processes and the higher order atomic correlation. In particular it has shown that the above mechanism, which produces the minimum of DOS, also causes the high resistivity. Furthermore it has been pointed out that the Mooij correlation comes partly from the same physical origin. Although we need to include higher angular momentum phase shifts for quantitative arguments, we think that the story is basically true for all s–p metals. In particular, it is emphasized that the essential physics of the transport processes near the DOS minimum lies in the short range order rather than the disorder, and so the quantum interference effect is not relevant. It seems to be paradoxical that the 'order' can increase the resistivity. This is however reasonable when one recalls that the Bragg reflection creates the band gap in the crystalline state; the effective mass of an electron becomes infinite and no conduction is allowed there. Generally speaking, the structure effect is considered to be more important than the localization effect in liquid or amorphous metals. It should be recalled that the success of the Ziman formula is totally dependent on the introduction of the structure factor; the structure effect is important even in the weak scattering case. If the individual scatterer has a large scattering amplitude, a slight change in the atomic structure must make a substantial change in the total scattering amplitude. The effect is therefore expected to be more pronounced in strong scattering materials and no definite conclusion can be derived without studying this effect. Some of the analysis made in the last section may hold even in the systems including the transition elements as major components. The Fermi level is expected to lie in the d-band in these systems, since the d-state can accommodate as many as ten electrons per atom, and the majority of the high resistivity metals are classified into this category. The conductivity function $\sigma(E)$ is then expected to have a deep minimum around the Fermi level, because the strong scattering due to resonance and hybridization is expected only in the narrow d-band. The negative TCR is therefore expected for those high resistivity metals through the smearing of the Fermi–Dirac distribution. In any case, our calculation shows that the temperature dependence of resistivity can possibly be explained without taking account of the electron–phonon interaction explicitly. This is in agreement with the conclusion obtained by Zhao and Ching from their simulation study. The thermoelectric power is obtained from the logarithmic derivative of $\sigma(E)$. This quantity is therefore very sensitive to the position of the Fermi level relative to the minimum position.

It is notable that the spectral functions have a sharp peak away from the minimum of the DOS, although the quantitative deviations of the resistivity values from the Ziman formula are still observed there. As stressed in section 3.2 the sharp peak of the spectral function indicates that the quasi-particle picture holds, and it implies that the Hall constant is free electron-like there (Itoh 1985). This is in complete agreement with the experimental results on the Hall constant of s–p metals (Häussler and Baumann 1983, Mizutani 1983). The deviation of the Hall constant from the NFE value, which is observed

only in the vicinity of $e/a \simeq 1.8$ is considered to be due to the strong damping and the double peak structure around $k = k_p/2$. It is impossible to interpret this deviation in terms of the dispersion effect only.

Finally, we make a few remarks on the points which have often caused misunderstandings in the literature. The problem is the definitions of the 'strong scattering metals' and the 'mean free path'. The latter is often estimated from the observed resistivity value using the Ziman formula with the free electron mass. The material is said to be strong scattering when the mean free path evaluated in this way becomes comparable to the interatomic distance. It is in fact self-contradicting to use the Ziman formula in such an extreme case. We emphasize that the magnitude of the resistivity is generally not directly related to the mean free path. For example, we can construct a perfect crystal by using very strong one-electron potentials. Introducing a slight deformation to this system would realize both the high resistivity (i.e. the short mean free path in the above sense) and the long relaxation time, with the enormous effective mass of an electron. The Boltzmann approach is still valid for a weak disorder, and the proper mean free path should be identified with the coherence length of the wave function at the Fermi energy. The tight binding model is a possible description for such a case and it is shown that a sufficiently long wave-coherence can result (Itoh and Watabe 1984a, Krey *et al* 1984). The above situation is markedly different from the NFE system, although the Hall constant is given by the free electron value. It must be noted that the free electron value of the Hall constant does not necessarily mean that the system is free-electron-like, but that the coherence length is long. The above physical picture should be important for the understanding of the systems with d- or f-electrons. Of course the damping effect will be equally important, and the Green function formalism incorporates both aspects, being capable of dealing with the 'strong scattering metals' in an unambiguous way.

As we have often emphasized, the EMA is a highly self-consistent formalism that includes the multiple scattering processes and the atomic short range order. Apart from the approximations included in the theory, it is a first principle calculation, requiring no adjustable parameters. It is also capable of dealing with various electronic properties on equal footings. Systematic studies are planned for future work.

Acknowledgment

The authors would like to express their gratitude to the Swiss National Science Foundation for financial support.

Appendix

The equations (1.1)–(1.3) are written in terms of the singular quantities B_k, $\tilde{B}_k$ and $\tilde{G}_k$. For numerical calculations we rewrite them in a divergence free form. For this purpose we introduce the regular part of $\tilde{G}_k$:

$$R_k(\kappa) = \tilde{G}_k(\kappa) - B_k(\kappa). \tag{A1}$$

Then, noting that

$$\tilde{B}_k(\kappa) = B_k(\kappa) + \int_0^\infty \frac{q^2\,\mathrm{d}q}{2\pi^2 n}\, a_0(k, q) B_q(\kappa) \tag{A2}$$

we obtain

$$R_k(\kappa) = \int_0^\infty \frac{q^2\,\mathrm{d}q}{2\pi^2 n} a_0(k,q) f(q)(n^{-1}Q_d^{-1} + R_q + B_q^{-1}R_q^2) \tag{A3}$$

$$\tau^{-1} - Q_d^{-1} = \int_0^\infty \frac{k^2\,\mathrm{d}k}{2\pi^2} R_k f(k) + \int_0^\infty \frac{k^2\,\mathrm{d}k}{2\pi^2} B_k f(k) \tag{A4}$$

where $f(k)$ is a non-singular function defined by

$$f(k) = B_k(\kappa)Q_k(\kappa,\kappa) = n(Q_d^{-1}B_k^{-1} - nR_kB_k^{-1} - n)^{-1}. \tag{A5}$$

The singular integration in the second term of (A4) can be further transformed as

$$\int_0^\infty \frac{k^2\,\mathrm{d}k}{2\pi^2} B_k f(k) = -\frac{1}{2\pi^2}\int_0^\infty \mathrm{d}k \frac{k^2 f(k) - \kappa^2 f(\kappa)}{k^2 - \kappa^2} - \frac{1}{2\pi^2}\int_0^\infty \mathrm{d}k \frac{\kappa^2 f(\kappa)}{k^2 - \kappa^2}$$

$$= -\frac{1}{2\pi^2}\int_0^\infty \mathrm{d}k \frac{k^2 f(k) - \kappa^2 f(\kappa)}{k^2 - \kappa^2} + \mathrm{i}\frac{\kappa}{4\pi} f(\kappa) \tag{A6}$$

and the integrand of the first term in the above expression is no more singular. Its evaluation at $k = \kappa$, however, requires the derivative of $f(k)$. This can be treated by the numerical differentiation or by setting up another equation for the differential quantity, which is to be solved simultaneously.

The divergence is removed because the free propagator always appears as a combination of (A5). For the conductivity calculation, it appears either with $Q_k(\kappa,\kappa)$ or with $(t(k,k') - t(k,\kappa)t(\kappa,k')/\tau)$; in any case, τ, the divergence, is suppressed.

References

Beck H, Frésard R and Cuche Y 1987 *Z. Phys.* B **68** 237

Ehrenreich H and Schwartz M A 1976 *Solid State Physics* vol 31, ed F Seitz and D Turnbull (New York: Academic) p 149

Frésard R 1989 Etude de la diffusion multiple des électrons dans les métaux désordonnés *Doctoral Thesis* University of Neuchâtel

Frésard R and Beck H 1986 *Physica* B **141** 243

Frésard R, Beck H and Itoh M 1990 *J. Non-Cryst. Solids* **117 + 118** 405

Fuda M and Whiting J 1973 *Phys. Rev.* C **8** 1255

Häussler P 1983 *Z. Phys.* B **53** 15

Häussler P and Baumann F 1983 *Z. Phys.* B **49** 303

Howson M A and Gallagher B L 1988 *Phys. Rep.* **170** 265

Huisman L, Nicholson D, Schwartz L M and Bansil A 1981 *Phys. Rev.* B **24** 1824

Itoh M 1985 *J. Phys. F: Met. Phys.* **15** 1715

Itoh M, Beck H and Frésard R 1989 *J. Phys.: Condens. Matter* **1** 6381 (referred to as paper I)

Itoh M, Frésard R and Beck H 1990 *J. Phys.: Condens. Matter* **2** 2687 (referred to as paper II)

Itoh M and Watabe M 1984a *J. Phys. F: Met. Phys.* **14** 1847

—— 1984b *J. Phys. F: Met. Phys.* **14** L9

Krey U, Jeshek R and Fembacher W 1984 *J. Non-Cryst. Solids* **61 + 62** 1161

Kujawski E and Lambert E 1973 *Ann. Phys., NY* **81** 591

Lloyd P 1967 *Prod. Phys. Soc.* **90** 207, 217

Mizutani U 1983 *Prog. Mater. Sci.* **28** 2

Niizeki K 1979 *J. Phys. F: Met. Phys.* **9** L185

Roth L 1974 *Phys. Rev.* B **9** 2476

Roth L and Singh V 1982 *Phys. Rev.* B **25** 2522

Yonezawa F, Roth L and Watabe M 1975 *J. Phys. F: Met. Phys.* **5** 435

Zhao G L and Ching W Y 1989 *Phys. Rev. Lett.* **62** 2511